Chalcogenide Letters Vol. 18, No. 1, January 2021, p. 11 - 22

IMPACT OF ERBIUM-DOPED ZINC TELLURITE GLASSES ON RAMAN SPECTROSCOPY, ELASTIC AND OPTICAL PROPERTIES

S. N. NAZRIN, M. K. HALIMAH*, F. D. MUHAMMAD, A. A. LATIF, A. S. ASYIKIN
Glass and Dielectric Lab, Department of Physics, Faculty of Science, University Putra Malaysia, 43400, Serdang, Selangor, Malaysia

In this study, the melt-quenching technique was employed to fabricate a series of zinc tellurite glass systems doped with erbium oxide. At room temperature, raman spectroscopy, elastic and optical measurements were utilized to analyse and report the result of prepared glass samples. The raman spectra displays the existence of structural units of tellurite networks such as trigonal bipyramid and trigonal pyramid. The elastic parameters including Debye temperature, mean velocity, acoustic impedance and softening temperature provide a fluctuating trend against the concentration of erbium oxide. The increment and decrement of these parameters can be explained by the 'competition' of non-bridging and bridging oxygen atoms. In the aspect of optical approach, the oxide ion polarizability, optical basicity and metallization criterion display more than one trend. Again, this can be correlated to the presence of erbium oxide which affects the vicinity in the glass matrix.

(Received September 3, 2020; Accepted January 13, 2021)

Keywords: Tellurite glass, Er_2O_3, Raman spectroscopy, Softening temperature, Oxide ion polarizability

1. Introduction

Erbium oxide is known as a material that has brought a huge potential in terms of optical application together with the aid of tellurite glasses [1,2]. The promising criteria for tellurite such as large linear and non-linear refractive index, small phonon energy, many valence states of tellurium, efficient infrared transmittance and chemical durability enhance the execution of fiber laser and optical amplifier devices [1-3]. Among many methods that have been suggested, Raman scattering is utilized to determine the information of the structure of the glasses specifically on the molecular units that exist in the lattice network of the atomic arrangement around the active rare-earth dopants.

Elastic parameters are another properties that are very crucial and informative in term of defining the structure and mechanical properties of the glasses. This is more efficient as they are influenced by the structural (softening/compactness), changes in geometrical configuration, dimensionality and cross-link density which can be attributed to the dopant that act as oxide modifier. In addition, the ultrasonic pulse-echo method has been inferred as convenient equipment to determine the elastic properties of glasses as a function of composition, frequency or temperature. According to earlier researchers [4-7], most ultrasonic investigation on tellurite glasses have focused on the changes in values of elastic moduli as well as Poisson's ratio with the density. The reliability of the composition towards elastic properties in the tellurite glasses is the condition that needs to be observed deeply.

The addition of two or more glass formers into the tellurite glasses can affect the optical properties of the materials in the field of scientific and technical applications at the same time. The desirable criteria of tellurite such as high non-linear refractive index, low melting point, low phonon energy which approximately lies from 700 to 800 cm^{-1} and larger refractive index of tellurite glasses as compared to other oxide glasses provide better outcome in obtaining a large rate off radiative transition of rare earth ions. Usually, tellurite glasses is utilized in the application of

* Corresponding author: hmk6360@gmail.com

optical fibers and planar waveguides. Meanwhile, the inclusion of zinc oxide into the glass samples is observed to help in reducing the rate of crystallization process as well as enhancing the glass forming ability [8-9].

Although some researches on the synthesis and characterization of tellurite glasses have been implemented, the use of erbium oxide has never been investigated. Plus, the evaluation on structural, elastic and optical properties of the glass system also have never been reported. Therefore, throughout this research, a glass system of erbium-doped zinc tellurite glasses were identified and characterized on structural, elastic and optical properties.

2. Experimental

A series of glasses were fabricated using oxide powders of tellurium (IV) oxide, TeO_2 (Aldrich 99.5%), zinc oxide, ZnO (Alfa Aesar 99.99%) and erbium (III) oxide, Er_2O_3 (Alfa Aesar, 99.9%) utilizing the melt-quenching method. The amount of calculated dopant was varied between 0.01 until 0.05 molar fractions of erbium oxide.

The mixture of all chemical powders that was mixed together was weighed by using an electronic weighing balance machine with an accuracy of $\pm$ 0.0001 g. The entire chemical with a weight of 11 g were completely blended and put into the alumina crucible. The glass rod, spatula and alumina crucible were cleaned earlier by using distilled water and acetone in order to prevent any impurities spotted on the equipment. Next, the mixture was consistently stirred for about 30 minutes to produce a homogenous mixture.

The homogenous mixture in the alumina crucible was positioned in the first furnace and heated at a temperature of 400℃. The mixture was kept at this temperature for one hour with a purpose to remove the water content in the mixture which will affect the final result. After one hour, the crucible was then transferred to the second furnace for two hours at 900℃. The mixture in the crucible was melted in this furnace. A stainless steel cylindrical shape split was used to mould the raw material which had been polished beforehand in order to get rid of the material from having any reaction with impurities on it. The stainless steel mould was also preheated at a temperature of 400℃ to avoid the thermal shock as a consequence of the temperature difference between the molten mixture and the mould. This process and melting process were done simultaneously at the same time.

The molten mixture that had been put into the mould was annealed at 400℃ for two hours. The aim of the annealing process is to remove the presence of air bubbles, discourage the thermal stress as well as to enhance the mechanical stress. The furnace was then switched off and the glass sample was allowed to cool down in the furnace at room temperature. The glass samples were taken out from the furnace and preserved in the bottle contained with silica gel to absorb any moisture [10].

The surfaces of the glass samples were polished by using SiC abrasive of grade 800, 1000, 1200, 2400 and 4000 in ascending order until a parallel, flat and smooth surface of the glass systems were attained. A vernier caliper was utilized to evaluate the thickness of glass sample and to study the thickness suitability for elasticity measurement which should be approximately 5.0 mm. On top of that, another prepared glass sample was measured around 2.3 mm in order to achieve an excellent optical measurement. Some parts of the glass samples were ground into powder by using the plunger. The glass samples were tested specifically for raman analysis.

3. Results and discussions

3.1. Raman spectroscopy

Fig. 1 displays the raman spectra of erbium-doped zinc tellurite glasses at room temperature. The doping concentration of the dopants ranges from 0.01 till 0.05 molar fractions. The shape of raman spectra was found having slightly similar to the previous reseachers who had also studied the tellurite glasses system as based glass [11-14]. In analyzing the raman spectra,

three distinct regions can be declared as shown in Fig. 1. It ranges around 120, 670,and 760 cm^{-1} at the respective wavenumber. The intensity also increases as the erbium concentration increases as observed in the figure.

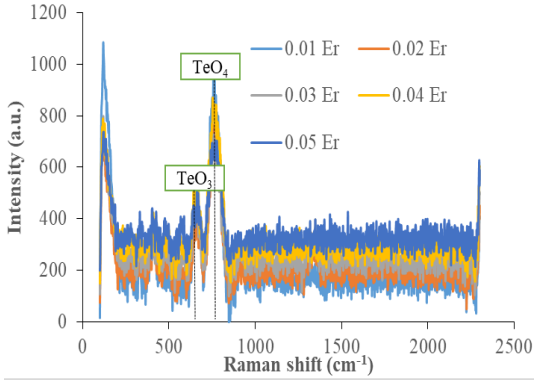

Fig. 1. Raman spectra of erbium-doped zinc tellurite glasses.

The investigation of the oxide modifier in the tellurite glasses are formed by a three dimensional network which is composed of asymmetrical TeO_4 trigonal bipyramids when the content of modifier is literally low [15]. The increment of concentration of oxide modifier enhances the creation of distorted TeO_{3+1} units where the subscript '3+1' indicates the presence of a longer bond compared to the other three [16] followed by the formation of trigonal pyramid (TeO_3) which is attributed to the formation non-bridging oxygen atoms (NBO) [17].

Based on 670 and 760 cm^{-1} observed in raman spectra, it can be assigned that those wavenumbers belong to the stretching vibration of trigonal bipyramid and trigonal pyramid or TeO_{3+1} units respectively. The increment intensity of the observed 760 cm^{-1} with erbium concentration is consistent with the destruction of trigonal bipyramid groups. The introduction of erbium oxide into the glass network encourage the reduction of tellurium coordination (4 to 3+1 to 3) which therefore lead to the substantial changes in the glass structure. According to Sekiya et al., (1995), Duverger et al., (1997) and Sakida et al., (1999) [13-15], the inclusion of erbium ions will perfectly give an impact to the Te-O local structure as well as can be deduced that the trigonal bipyramid can be converted into trigonal pyramid as the number of erbium ions incline in the glass network.

Referring to 425 cm^{-1}, it is usually can be explained by the bending vibrations of Te-O-Te linkages [18-20] which is also created by the vertex sharing of TeO_4, TeO_{3+1} and TeO_3 polyhedra. As can be seen from Figure 1, the decrease of the intensity of these bands TeO_4, TeO_{3+1} and TeO_3 with the increment of dopant concentration unveils that the erbium deforms the Te-O-Te linkages. Moreover, the decrement of intensity of 425 cm^{-1} can be attributed to the presence of erbium ions in tellurite glasses that break down the Te-O-Te linkage and produce numbers of non-bridging oxygen atom. This can be further supported with the conversion of trigonal bipyramid into trigonal pyramid having one NBO atoms. Therefore, the inclusion of erbium oxide into tellurite based glasses breaks the Te-O-Te bonds and leads to the decrement in the Te coordination number. Meanwhile, at 120 cm^{-1}, it can be associated with the rotational and torsional modes of the vibrations of TeO_4-ZnO_6-TeO_3 chain structures. Specifically, Zn plays a role as a glass network forming in agreement with the vibrational frequencies of $ZnTeO_3$ and $Zn_2TeO_3O_8$ crystals [21].

Table 1. Debye temperature, θ_D, mean velocity, v_{mean}, acoustic impedance, Z and softening temperature, T_s, of erbium-doped zinc tellurite glasses.

Elastic parameter	0.01	0.02	0.03	0.04	0.05
θ_D (K)	249.65	245.70	246.28	246.78	270.18
v_{mean} (m/s)	2055.00	2024.30	2033.41	2045.94	2037.13
Z (x10^7 kg/m^{2}s)	1.797	1.794	1.832	1.845	1.859
T_s (K)	386.82	378.24	383.54	393.91	392.10

3.2. Elastic properties

From the elastic data, there are other parameters that can be evaluated which are Debye temperature, mean velocity, acoustic impedance and also softening temperature. Debye temperature is a parameter that is related to atomic vibration and highly affected by mean ultrasonic velocity. In the meantime, it is also presenting the temperature at which all modes of vibrations in solid are excited. This parameter can be influenced by the number of vibrating atoms per unit volume (N/V) and its escalation indicates the increment in the rigidity of a glass system. In this investigation, Debye temperature can be evaluated by using the equation below:

$$\theta_D = \frac{h}{k}\left(\frac{3N_A}{4\Pi V_m}\right)^{\frac{1}{3}} v_{mean}^{\frac{-1}{3}} \quad (1)$$

where θ_D is the Debye temperature, h, k, N_A and Π is equivalent to $6.626x10^{-34}J.s$, $1.381x10^{-23}J.K^{-1}$, $6.023\,x\,10^{23}$, and 3.142 respectively, V_m is molar volume and v_{mean} is the mean ultrasonic velocity. v_{mean} is identified using the following relations:

$$v_{mean} = \left[\frac{1}{3}\left(\frac{2}{v_s^3} + \frac{1}{v_L^3}\right)\right]^{\frac{-1}{3}} \quad (2)$$

The increment of Debye temperature has brought a tendency to elevate the connectivity and compactness of a glass network while the bonds are tightly associated and improve in their covalence. Indirectly, it will cause the glass rigidity to increase.

Besides that, the acoustic impedance is a measurement of transmission and reflection of sound energy in the glass specimen. It relies on the sound velocity (v_L) and also the density (ρ) of a material. High acoustic impedance signifies that the rigidity and connectivity of a sample tend to be increased. Other than that, the acoustic impedance also defines the tendency of sound to transmit in two different materials. As sound passes through two different materials that connected together, it is crucial for those materials to have little differences in their acoustic impedance. This is due to the fact that sound energy will be reflected as it encounters a material with different acoustic impedance. The relation that can be used to calculate this parameter is as shown below:

$$Z = v_L\rho \quad (3)$$

where Z is the acoustic impedance. Based on the equation, it can be said that a denser material will have higher Z and vice versa.

Softening temperature is defined as the temperature in which a material softens as it is dominated to heat. This parameter can be evaluated using the following equation.

$$T_s = \frac{v_s^2 M_T}{c^2 P} \quad (4)$$

where T_s is the softening temperature and c is a constant which equivalent to 0.5074 x 10^5 cm/sK^{-1}. As the rigidity of material increases, it is expected for this parameter to increase as well. In contrast, the decrement of T_s indicates that the glass network becomes less tightly packed and

more non-bridging oxygen will form. As a result, the bonds between the atoms will become weaker and the amount of energy needed to break the bonds and soften the material will be smaller.

3.3. Debye temperature and mean velocity

Fig. 2 displays the diversity of Debye temperature (θ_D) and mean velocity with the inclusion of erbium oxide inside the glass system. Debye temperature describes the temperature where all high—frequency of the lattice vibrational modes are excited. Some of the researchers, Saddeek (2004), Gaafar et al., (2009), Marzouk, (2010) and Elokr and AbouDeif (2016) [22-25] had reported that Debye temperature is one of the parameter that is used to investigate the characteristics of the solid materials which is correlated to the atomic vibration in the glass network.

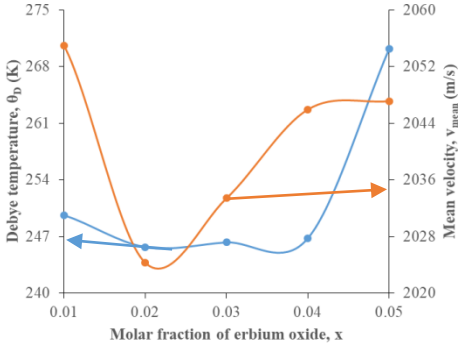

Fig. 2. Debye temperature (K) and mean velocity of erbium-doped zinc tellurite glasses.

Fig. 2 illustrates the graph of Debye temperature (θ_D) and mean velocity against the concentration of erbium-doped zinc tellurite glass system. Earlier researchers had reported that Debye temperature is correlated to the mean ultrasonic velocity (v_{mean}). The elevation of Debye temperature entails the rise in the ultrasonic velocity and also encourages the strength of the glass network structure [26]. This can be elaborated more by the increment of the number of bond per unit volume that is strongly related to the connectivity of the glass network structure [27].

In the meantime, the decrement of Debye temperature can be related to the creation of non-bridging oxygen in the glass network. As mentioned in the raman spectra section, it is observed that there is a presence of trigonal bipyramid and trigonal pyramid where the conversion of these structural units leads to the formation of non-bridging oxygen. Saddeek (2004) [22] had proposed that the glass structure becomes less compact and reduce in the rigidity as the lattice vibration start to decrease. In addition, the declination of bond strength is another crucial factor that promotes the decrement in Debye temperature. Molecular vibration in the network structure can be noticed as spring vibration where the force needed to move the molecules is dependent to the bond strength. As the bond strength of the glass structure reduces, it will be easier for the atoms to vibrate and the energy needed to do will also decline. Therefore, this will reduce the amount of Debye temperature of the glasses [28]. The decrement in Debye temperature might also be due to the decrease of the ultrasonic velocities that lead to the formation of more non-bridging oxygen as mentioned by Nazrin et al., (2018) [29].

3.4. Acoustic impedance

Acoustic impedance or specific acoustic impedance measures the opposition that a system presents to the acoustic flow resulting from an acoustic pressure applied to the system. Figure 3 shows the graphs of acoustic impedance (Z) with respect to the molar fraction of erbium oxide. From the figure, it can be observed that the acoustic impedance increases as more dopants are added into the glass system. The trend probably can be attributed to larger cross-link density and number of bond per unit volume. In details, larger cross-link density and larger number of bond

per unit volume lead to the higher of acoustic impedance which may be caused by the numbers of bridging oxygen within the glass system.

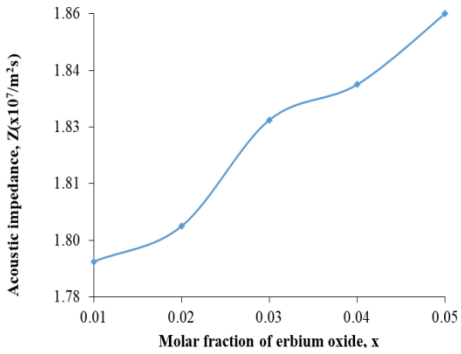

Fig. 3. Acoustic impedance, Z of erbium-doped zinc tellurite glasses.

3.5. Softening temperature

Softening temperature (T_s) is another parameter that can be evaluated using the shear velocity data. It has a tendency to discard some light on the temperature where the glass starts to soften when exposed to the heat. This is significant to investigate the temperature stability of the glass. Other than that, the need of the glass to have small or large softening temperature is also dependable on its applications. If the glass used is at higher temperature, therefore, the glass requires high softening temperature in order to avoid it from soften. In contrast, the small amount of softening temperature is beneficial to shape the glass especially in the curved glass industry.

Softening temperature is observed to increase, decrease and increase (fluctuating trend) at particular concentration of erbium-doped zinc tellurite glasses as can be observed in Figure 4. Halimah *et al.*, (2010) [30] and Bootjomchai, (2015) [31] had reported that the declination of softening temperature which is due to the inclusion of dopants in the glass system promotes lesser tightly packed of glass network structure which then results in the creation of non-bridging oxygen atoms (NBOs). As a consequence, less energy is required to break the bonds within the glass system. This can be observed in the figure where the decrement of softening temperature can be supported by the conversion of trigonal bipyramid into trigonal pyramid as illustrated in raman spectra section.

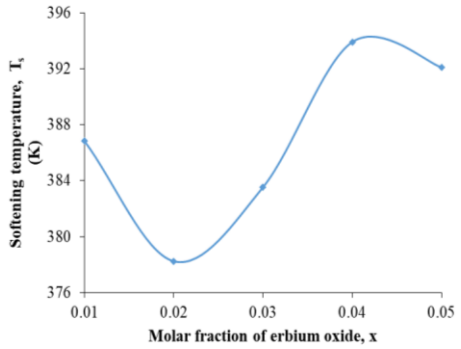

Fig. 4. Softening temperature of erbium-doped zinc tellurite glasses.

Another point that affects the changes of the softening temperature is the micro-hardness of the glasses which had been mentioned by Nazrin et al., (2018) [29]. The increment of micro-hardness eventually will strengthen the softening points of the glass. Therefore, the softening temperature is predicted to increase as the micro-hardness increases or vice versa. The maximum point of softening temperature is usually affected by the inclination of shear velocity of the glass

samples at specific concentration. Hence, the increment of shear velocity will cause the softening temperature to increase [29].

4. Optical properties

4.1. Oxide ion polarizability

Dimitrov and Sakka, (1996) [32] had proposed the evaluation of oxide ion polarizability on the basis of optical band gap energy. The deformability of the electron cloud of the oxide ion is greater than those of the cation. This can be associated by high capability of the cation electron to hold onto the cationic charge. As an outcome, the electron cloud of the cation will not polarize. The rapport between $\sqrt{E_g}$ and $1 - R_m/V_m$ was approached by Duffy, (1993) [34] for a large number of simple oxides from the following expression:

$$E_g = 20(1 - \frac{R_m}{V_m})^2 \quad (5)$$

The oxide ion polarizability can be attained by replacing the Equation (5) into Equation (6) as displayed by the following formula:

$$\alpha_{o_2-}(E_g) = [\frac{V_m}{2.52}\left(1 - \sqrt{\frac{E_g}{20}}\right) - \sum \alpha_i](N_{o_2-})^{-1} \quad (6)$$

It has been acknowledged that this equation is agreeable with the heavy metal oxide glasses.

Table 2. Oxide ion polarizability, optical basicity and metallization criterion of erbium-doped zinc tellurite glasses.

Optical parameters	0.01	0.02	0.03	0.04	0.05
Oxide ion polarizability, $\alpha_{O^{2-}}$	2.986	3.076	3.001	3.000	3.061
Optical basicity, Λ	1.111	1.127	1.114	1.113	1.124
Metallization criterion, M	0.387	0.374	0.383	0.384	0.369

4.2. Optical basicity

The chemical cooperation between the components of the oxide glasses consists of acid-based character. Based on the Lewis theory, a base consists at least one pair of valence electron that is not being shared by other molecules. At the same time, an acid contains of a vacant orbital can be accommodated by the other ions. In term of oxide glass system, the oxides play a role as a Lewis base and the metal acts like a Lewis acid. In addition, the negativity of the oxygen ions produces larger capability to transfer their negative charge to the cations. It is concern to study the tendency of the oxygen to transfer the negative charge to the surrounding of weak cations. A deep considerate of optical basicity was proposed by Duffy and Ingram, (1971) [34] from the experimental shift of the ultraviolet spectrum of a probe incorporated in various oxides.

Duffy and Ingram, (1971) [34] had also proposed the theoretical calculation of the optical basicity for the multi-component oxide glasses. Optical basicity can be identified as the numerical expression of the average electron donor power of the oxide species constituting the medium [35]. There is a compelling equality in physical background between oxide ion polarizability and optical basicity. The increment of oxide ion polarizability brings significance to the increase of electron

donor power. The optical basicity could be anticipated from the glass compositions and from the basicity moderating parameters of difference cations present [36].

The optical basicity can be evaluated by the following expression:

$$\Lambda = X_1\Lambda_1 + X_2\Lambda_2 + \ldots\ldots + X_n\Lambda_n \quad (7)$$

where $X_1, X_2, \ldots\ldots, X_n$ is the equivalent fractions of each oxide in which contributes to the overall material stoichiometry and $\Lambda_1, \Lambda_2, \ldots\ldots, \Lambda_n$ correspond to the optical basicity of each individual oxides in the glass system. The liaison between oxide ion polarizability and optical basicity can be noted by the following equation:

$$\Lambda = 1.67\left(1 - \frac{1}{\alpha_{o^{2-}}}\right) \quad (8)$$

The above correlation displays that the optical basicity increases with an increment of oxide ion polarizability.

4.3. Metallization criterion

The approach of the metallization of condensed matter can be clarified by the theory reported by Dimitrov and Komatsu (1999) [37]. The condition of $R_m/V_m = 1$ in the Lorentz-Lorenz equation proposed that the refractive index becomes continuous. This is in agreement with the metallization of covalent solid materials. In addition, the electrons will become itinerant and acquires metallic status [38]. The nature of metallic and non-metallic of oxide glasses can be anticipated by the following conditions: $R_m/V_m < 1$ (non-metal) and $R_m/V_m > 1$ (metal). Subtracting by 1 gives the equation of metallization criterion as shown in the following expression:

$$M = 1 - \frac{R_m}{V_m} \quad (9)$$

This equation shows that when the metallization criterion becomes zero, the transition process to the metal states will take place. The metallization criterion on the basis of refractive index and optical band gap can be evaluated by transform the Equation (9) to the following expression:

$$M = 1 - \frac{(n^2-1)}{(n^2+2)} = \left(\frac{E_g}{20}\right)^{1/2} \quad (10)$$

Dimitrov and Komatsu, (2010) [39] had proposed that a huge amount of glass-forming oxide leads to the increment of the metallization criterion [40]. High number of metallization criterion indicates that the width of the valence gap and conduction gap becomes smaller and leads to the expansion of the width of the band gap. This will result in the tendency for metallization of the glass system to decrease. Whereas, the materials which possess a large metallization criterion, M value close to 1 is said to be insulators.

4.4. Oxide ion polarizability

'The deformability of electron cloud of oxide ions is larger than cations'. This phenomenon occurs when the cations are tightly bound to the cationic surroundings. As a consequence, the values of cations polarizability are consistent with different compositions and compounds. However, the polarizability of oxide ions is inconsistent and varies widely. Therefore, it is vital to study the effect of erbium oxide concentration on the oxide ion polarizability. The graph of oxide ion polarizability of erbium oxide is depicted in Fig. 5.

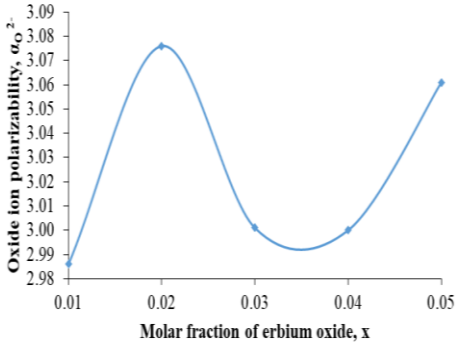

Fig. 5. Variation of oxide ion polarizability of erbium-doped zinc tellurite glasses.

Based on Fig. 5, a general increment of oxide ion polarizability except for 0.03 molar fractions of erbium oxide is observed. This can be attributed to the structural changes in the glass system as the concentration of dopants increase. The oxide ion polarizability can be explained by the influence of the changes in optical band gap energy as mentioned by Nazrin et al., (2018) [29]. The decrement in optical band gap promotes the increase of oxide ion polarizability [39]. On top of that, the increment of oxide ion polarizability is due to the breaking bond tellurite network when the erbium ions are inserted into the glass system which creates numbers of non-bridging oxygen atoms. The presence of non-bridging oxygen atoms enhance large polarizability and this occurrence can be supported by large bond length of erbium oxide and high atomic radius that create more spaces within the glass network [41].

4.5. Optical basicity

Theoretically, the optical basicity (Λ) is a measurement of electron donor power of anions in a medium. The anions in this current research refer to the oxygen ions since all the chemicals used are in oxide forms. Besides that, it is also stated by Elkhoshkhany *et al.*, (2014) [42] that this parameter helps in the estimation on the type of bonding that exists in a glass network. This can be associated with the formation of bonds in the glass system that is dependent on the donation or sharing of electrons. Therefore, as the electron donor power and Λ increases, the formation of ionic bonding will increase, causing the glass to become more basic. The reduction of electron donor power tends to produce more covalent bonding and the glass will become more acidic.

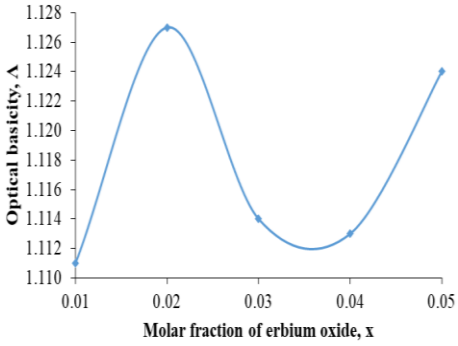

Fig. 6. Variation of molar refraction of erbium-doped zinc tellurite glasses.

As shown in Fig. 6, the optical basicity increases except for 0.03 molar fractions of erbium oxide. The increasing values of optical basicity indicate the increment of the oxides to donate electrons. The covalence of the glass network increases as the optical basicity increases. Currently, Dimitrov and Komatsu, (2010) [39] had evaluated the values of optical basicity for single component oxide specifically in erbium-doped glasses where the values of optical basicity for each

element of the present glass system are listed as follows: $\Lambda(Er_2O_3)$=0.929, $\Lambda(TeO_2)$=0.93 and Λ(ZnO)=0.82. It can be observed that optical basicity of tellurite oxide and erbium oxide is slightly the same. Zinc oxide is observed to have less basicity compared with other oxides. Because of high value of optical basicity of the dopants, the overall optical basicity in the glass system start to increase. High values of average optical basicity show the glass series to be more ionic and make the glass series becomes more basic. Meanwhile, when the glass system exhibits less optical basicity, the glass system tends to become more covalence and acidic.

In addition, the increment of the optical basicity can be attributed to the inclination of glass polarizability and improve the numbers of non-bridging oxygen (NBOs) within the glass system. As the NBOs increase, the ionic bonding prevails which will cause the glass to become more basic. This can be affirmed by the formation of TeO_3 structural units as mentioned in the part of raman spectra. Besides that, Lakshminarayana *et al.*, (2008) [43] had also stated that the increment of NBOs results in the inclination of negative charges around the cation and consequently increases the optical basicity of the glasses. Other than that, polarizability (α) and Λ are interrelated where both of these parameters are directly proportional to one another. The fact that polarization define the distortion of the electron cloud of an anion towards a cation, therefore, as the electron donor power of oxygen ions or optical basicity increases, the tendency of the polarization process to occur also becomes easier. Other than that, the other factor that could result in the inclination of Λ is the weaker bond strength of the dopants as stated by Duval *et al.*, (1990) [44].

4.6. Metallization criterion

Metallization criterion (M) parameter provides an overview regarding the electrical conduction ability of a glass sample. All the values which are more than zero indicate the insulating behaviour of the glasses and it is related to the optical band gap (E_{opt}) of the glass sample [45]. The plotted graph of metallization criterion against concentration is displayed in Figure 7. The relationship between metallization criterion and refractive index can be made by comparing the values. Earlier works by Nazrin et al., (2018) [29], there is an inverse relationship between refractive index and metallization criterion (current work). This indicates that a smaller value of refractive index leads to a higher value of metallization criterion. On top of that, the increment in metallization criterion can be attributed to the increment of optical band gap. This can be attributed to the decreasing number of free electrons with the increasing value of energy band gap. High value of metallization criterion shows that the glass series are not good conductor which is shown in certain concentration of erbium oxide. Therefore, it can be justified that the presence of erbium oxide tends to increase the M parameter of the glass system.

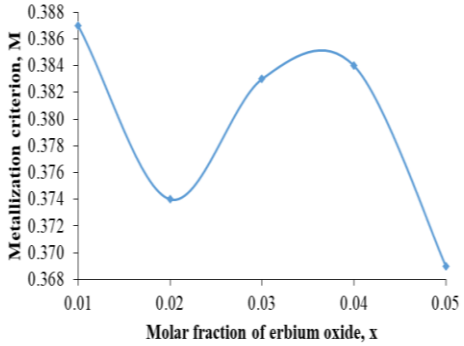

Fig. 7. Variation of metallization criterion of erbium-doped zinc tellurite glasses.

At certain concentration of erbium oxide which is from 0.01 to 0.02 molar fraction and from 0.04 to 0.05 molar fraction, the metallization criterion parameter is observed to decrease slightly. This can be explained by the increasing number of refractive index and the decreasing number of optical band gap as ascribed by Nazrin and other co-authors in 2018 [29]. Lack

presence of free electrons in the glass system promotes higher value of metallization criterion. Scientifically, when M is equivalent or approaching zero, the glass sample is said to achieve the metal state. Therefore, the continuous reduction of M as erbium oxide is added into the glass system suggests that the glass sample exhibits lesser insulating behaviour. The reduction of metallization criterion indicates that the valence and conduction bands become wider and therefore reduce the optical band gap [42]. The fact that the value of metallization criterion ranges in between 0.35-0.45, the glass samples are good to be used as non-linear application [46].

6. Conclusion

A series of zinc tellurite glasses doped with erbium oxide with chemical formula $[(TeO_2)_{0.7}(ZnO)_{0.3}]_{1-x}(Er_2O_3)_x$ where x = 0, 0.01, 0.02, 0.03, 0.04 and 0.05 was synthesized by utilizing melt-quenching method. Precisely, raman analysis shows the presence of the trigonal bipyramid and trigonal pyramid in the glass system. The elastic parameters such as Debye temperature, mean velocity, acoustic impedance and softening temperature display a fluctuating trend as expected.

The formation of bridging oxygen that creates stronger connectivity and rigidity of the glasses can be associated with the inclination of all the values of the elastic parameters. Meanwhile, the decreasing value of the related moduli can be attributed by the conversion of bridging oxygen into non-bridging oxygen which can be explained by the distortion of the bonds within the glass network. Eventually, this phenomena will reduce the rigidity and connectivity of the glass a network. Elastic properties might also be influenced by the structural changes that assign the variation of the molar fraction of the dopant. For theoretical optical approach, oxide ion polarizability, optical basicity and metallization criterion were analysed as well. The variation trend of the oxide ion polarizability and optical basicity is similar where this phenomena can be attributed to the formation of non-bridging oxygen atoms which are more polarizable than bridging oxygen atoms.

The effect of large concentration of rare earth ions, Er^{3+} ions creates denser packing structure of rare earth modifiers in the host glass material and the effect of size of cation Er^{3+} has the highest polarizability value among other elements. Meanwhile, the metallization criterion is to have opposite characteristic compared to the aforementioned optical parameters. Higher metallization criterion can be explained by the existence plenty of non-bridging oxygen atoms within the glass matrix.

Acknowledgements

The financial support from UPM through the research Grant Putra (IPS) 9642300 is gratefully acknowledged.

References

[1] S. Sudo, Optical fiber amplifiers: materials, devices, and applications. Artech house, 1997.
[2] M. J. Digonnet, (Ed.), Rare-earth-doped fiber lasers and amplifiers, revised and expanded, CRC press, 2001.
[3] E. Desurvire, E. D. F. Amplifiers, John Wiley & Sons. New York, 1994.
[4] R. Ota, N. Soga, Journal of Non-Crystalline Solids **56**(1-3), 105 (1983).
[5] A. N. Begum, V. Rajendran, Journal of Physics and Chemistry of Solids **67**(8), 1697 (2006).
[6] A. N. Begum, V. Rajendran, Materials letters **61**(11-12), 2143 (2007).
[7] X. Zhao, H. Kozuka, S. Sakka, Journal of materials science **22**(11), 4103 (1987).
[8] K. Selvaraju, K. Marimuthu, Journal of luminescence **132**(5), 1171 (2012).
[9] P. G. Pavani, K. Sadhana, V. C. Mouli, Physica B: Condensed Matter **406**(6-7), 1242 (2011).
[10] S. N. Nazrin, M. K. Halimah, F. D. Muhammad, Journal of Materials Science: Materials in

Electronics **30**(7), 6378 (2019).
[11] H. Li, Y. Su, Y., & Sundaram, Journal of non-crystalline solids **293**, 402 (2001).
[12] Y. C. Boulmetis, A. Perakis, C. Raptis, D. Arsova, E. Vateva, D. Nesheva, E. Skordeva, Journal of non-crystalline solids **347**(1-3), 187 (2004).
[13] T. Sekiya, N. Mochida, A. Soejima, Journal of non-crystalline solids **191**(1-2), 115 (1995).
[14] C. Duverger, M. Bouazaoui, S. Turrell, Journal of non-crystalline solids **220**(2-3), 169 (1997).
[15] S. Sakida, S. Hayakawa, T. Yoko, Journal of Non-Crystalline Solids **243**(1), 13 (1999).
[16] J. C. Sabadel, P. Armand, P. E. Lippens, D. Cachau-Herreillat, E. Philippot, Journal of non-crystalline solids **244**(2-3), 143 (1999).
[17] J. C. Sabadel, P. Armand, F. Terki, J. Pelous, D. Cachau-Herreillat, E. Philippot, Journal of Physics and Chemistry of Solids **61**(11), 1745 (2000).
[18] S. Khatir, F. Romain, J. Portier, S. Rossignol, B. Tanguy, J. J. Videau, S. Turrell, Journal of molecular structure **298**, 13 (1993).
[19] H. Bürger, K. Kneipp, H. Hobert, W. Vogel, V. Kozhukharov, S. Neov, Journal of non-crystalline solids **151**(1-2), 134 (1992).
[20] Y. H. Wang, A. Osaka, Y. Miura, J. Takada, K. Oda, K. Takahashi, Materials Science Forum **32**, 161 (1988).
[21] M. Mazzuca, J. Portier, B. Tanguy, F. Romain, A. Fadli, S. Turrell, Journal of molecular structure **349**, 413 (1995).
[22] Y. B. Saddeek, Materials Chemistry and Physics **83**(2-3), 222 (2004).
[23] M. S. Gaafar, N. A. El-Aal, O. W. Gerges, G. El-Amir, Journal of Alloys and Compounds **475**(1-2), 535 (2009).
[24] S. Y. Marzouk, Physica B: Condensed Matter **405**(16), 3395 (2010).
[25] M. M. Elokr, Y. M. AbouDeif, Journal of Molecular Structure **1108**, 257 (2016).
[26] N. A. El-Aal, Egypt. J. Sol. **24**, 181 (2001).
[27] H. A. Al-Shamiri, A. S. Eid, Photonics and Optoelectronics **1**(1), 1 (2012).
[28] Y. B. Saddeek, Materials Chemistry and Physics **91**(1), 146 (2005).
[29] S. N. Nazrin, M. K. Halimah, F. D. Muhammad, J. S. Yip, L. Hasnimulyati, M. F. Faznny, I. Zaitizila, Journal of Non-Crystalline Solids **490**, 35 (2018).
[30] M. K. Halimah, W. M. Daud, H. A. A. Sidek, A. W. Zaidan, A. S. Zainal, Materials Science-Poland **28**(1), 173 (2010).
[31] C. Bootjomchai, Radiation Physics and Chemistry **110**, 96 (2015).
[32] V. Dimitrov, S. Sakka, Journal of Applied Physics **79**(3), 1736 (1996).
[33] J. A. Duffy, Geochimica et Cosmochimica Acta **57**(16), 3961 (1993).
[34] J. A. Duffy, M. D. Ingram, Journal of the American Chemical Society **93**(24), 6448 (1971).
[35] T. Inoue, T. Honma, V. Dimitrov, T. Komatsu, Journal of solid state chemistry **183**(12), 307810).
[36] M. Abdel-Baki, F. El-Diasty, F. A. A. Wahab, Optics communications **261**(1), 65 (2006).
[37] V. Dimitrov, T. Komatsu, Journal of non-crystalline solids **249**(2-3), 160 (1999).
[38] X. Zhao, X. Wang, H. Lin, Z. Wang, Physica B: Condensed Matter **390**(1-2), 293 (2007).
[39] V. Dimitrov, T. Komatsu, J. Univ. Chem. Technol. Metall. **45**(3), 219 (2010).
[40] V. Dimitrov, T. Komatsu, Journal of solid state chemistry **178**(3), 831 (2005).
[41] Z. A. S. Mahraz, M. R. Sahar, S. K. Ghoshal, Journal of Molecular Structure **1072**, 238 014).
[42] N. Elkhoshkhany, R. Abbas, R. El-Mallawany, Ceramics International **40**(8), 11985 (2014).
[43] G. Lakshminarayana, R. Yang, J. R. Qiu, M. G. Brik, G. A. Kumar, I. V. Kityk, Journal of Physics D: Applied Physics **42**(1), 015414 (2008).
[44] E. Duval, A. Boukenter, T. Achibat, Journal of Physics: Condensed Matter **2**(51), 10227 (1990).
[45] M. K. Halimah, S. N. Nazrin, F. D. Muhammad, Chalcogenide Letters **16**(8), 2019.
[46] C. Eevon, M. K. Halimah, A. Zakaria, C. A. C. Azurahanim, M. N. Azlan, M. F. Faznny, Results in physics **6**, 761 (2016).